

ASIAN JOURNAL OF ORGANIC CHEMISTRY

www.asianjoc.org

Accepted Article

Title: Butyrylcholinesterase responsive supramolecular prodrug with targeted near-infrared cellular imaging property

Authors: Yu Liu, Yonghui Sun, Yong Chen, and Xianyin Dai

This manuscript has been accepted after peer review and appears as an Accepted Article online prior to editing, proofing, and formal publication of the final Version of Record (VoR). This work is currently citable by using the Digital Object Identifier (DOI) given below. The VoR will be published online in Early View as soon as possible and may be different to this Accepted Article as a result of editing. Readers should obtain the VoR from the journal website shown below when it is published to ensure accuracy of information. The authors are responsible for the content of this Accepted Article.

To be cited as: *Asian J. Org. Chem* 10.1002/ajoc.202100541

Link to VoR: <https://doi.org/10.1002/ajoc.202100541>

A Journal of



A sister journal of *Chemistry – An Asian Journal*
and *European Journal of Organic Chemistry*

WILEY-VCH

Butyrylcholinesterase responsive supramolecular prodrug with targeted near-infrared cellular imaging property

Yonghui Sun,^[a] Yong Chen,^[a] Xianyin Dai,^[a] and Yu Liu ^{*[a,b]}

[a] Yonghui Sun, Dr. Yong Chen, Xianyin Dai, Prof. Y. Liu
College of Chemistry, State Key Laboratory of Elemento-Organic Chemistry,
Nankai University, Tianjin 300071, China
E-mail: yuliu@nankai.edu.cn

[b] Prof. Y. Liu
Collaborative Innovation Center of Chemical Science and Engineering
(Tianjin), Tianjin 300072, China

Supporting information for this article is given via a link at the end of the document.

Abstract: An enzyme responsive supramolecular prodrug with near-infrared targeted cell imaging property is constructed from organic dye (4-(3-(benzo[d]thiazol-2-yl)-2-hydroxy-5-methylstyryl)-1-methylpyridin-1-ium) (G), anti-cancer drug chlorambucil (Cbl-G), water-soluble cucurbit[7]uril (CB[7]) and biocompatible hyaluronic acid (HA). It is very interesting that CB[7] can not only associate Cbl-G to form supramolecular nanofibers, but also further assemble with targeter HA to form supramolecular nanoparticles with a diameter of about 200 nm. The loading efficiency of Cbl-G in the assembly is calculated to be as high as 98.2%. Cell experiments using HeLa and A549 cancer cells indicated that the prodrug nanoparticles are easily internalized into cancer cells via receptor-mediated endocytosis, and disassembled under the action of butyrylcholinesterase by cutting the ester bond of prodrug, exhibiting a controlled drug release behavior as well as a simultaneous near-infrared (NIR) fluorescence imaging in cancer cells. The present research might provide a feasible strategy for in situ monitoring drug delivery and NIR cellular imaging.

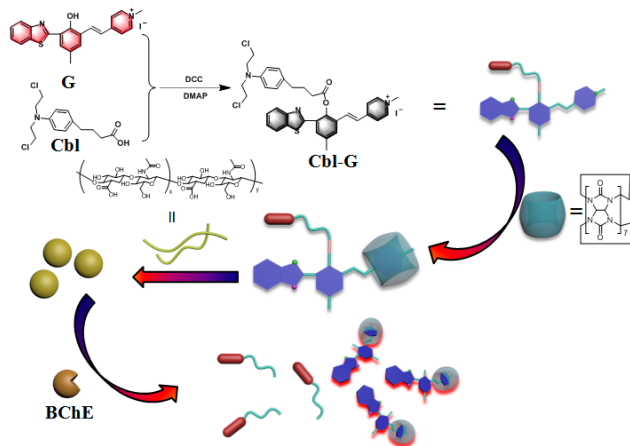
Enzyme-responsive supramolecular assemblies constructed from macrocyclic compounds have become research hot-spot in the field of drug delivery and bioimaging in recent years.¹ By intelligently controlling the dissociation of the assembly, the delivery of cargo can be effectively realized.² Recently, many classes of macrocycles have been used in pharmaceutical practice, and they provide interesting functions in the design of new therapy and drug delivery methods.³ Among them, cucurbit[n]urils (CBs, n=5-8, 10, 14), a family of macrocyclic host molecules with a hydrophobic cavity created from acid-catalyzed polymerization of glycouril and formaldehyde, are widely focused owing to the ability of fabricating stable inclusion complexes with cationic guest molecules.⁴ In addition, cucurbiturils, specifically CB[7], show good water solubility and can assemble with many guest molecules driven by the ion-dipole interaction between positively charged atoms on guest molecules and carbonyl oxygens on the rims of CB[7], and this binding affinities are many orders of magnitude higher than the same guest molecules with cyclodextrin.⁵ To date, CB[n] and its derivatives have been widely used in constructing stimuli-responsive supramolecular drug delivery systems (SDDSs) or targeted cellular imaging.⁶ For instance, we used cucurbituril and amphiphilic calixarene to construct a two-stage mediated near-infrared (NIR) emission supramolecular assembly for lysosomal-targeted cell imaging.⁷ Ma et al. reported acid labile acyclic CB[n] molecular containers that could encapsulate anti-tumor drugs and control drug release under mildly acidic conditions in live cells. In addition, CB [n] also show many practical superiorities in drug delivery and bioimaging, including ease to fabrication, molecular-level protection,

sensitive stimulus response and traceless release. Isaacs et al. reported a cubooctahedral metal organic polyhedron (MOP) functionalized with CB[7] units. In this system, complexation of the CB [7] unit with the alkanediammonium ions functionalized with hydrophobic tails creates a hydrophobic nanoenvironment that can take up fluorescent dye Nile Red (NR) or anti-tumor drug doxorubicin (DOX), and the microenvironment can be destroyed in response to multiple stimuli, resulting in the simultaneous release of DOX or NR.⁸

On the other hand, hyaluronic acid (HA), which have outstanding hydrophilic motif with excellent aqueous solubility, have attracted significant attention in targeted drug delivery systems due to its biocompatibility, biodegradability, low toxicity, facile modification, and specific binding with CD44 and RHAMM receptors overexpressed on the surface of malignant cancer cells.⁹ For example, Cheng et al. reported aptamer and peptide-functionalized hyaluronic acids used as a delivery system to target cancer cells. By knocking out the CTNBN1 gene encoding β -catenin, it reverses the PD-L1-mediated cancer immune escape and immunosuppression, making it anti-tumor immunity is effectively restored.¹⁰

Therefore, it can be imagined that the incorporation of targeting units and stimulus-responsive prodrugs with CB[n] could provide real-time therapy monitoring and targeted treatment effects in the field of medicine. Even though numerous studies have been reported in this field, there are relatively few reports of SDDSs that simultaneously possess controlled drug release and near-infrared cell imaging abilities. Herein, a targeting drug delivery system with NIR cellular imaging and butyrylcholinesterase-responsive properties was rationally designed in a two-step assembly strategy. Firstly, NR-modified anti-cancer drug chlorambucil (Cbl-G) was synthesized through an esterification reaction. Due to the destruction of excited-state intramolecular proton transfer (ESIPT), the fluorescence of NIR was quenched.¹¹ After the formation of a supramolecular complex with CB[7], the binary assembly could further assemble to nanoparticles with an average diameter of around 200 nm under the action of hyaluronic acid (HA). On the other hand, butyrylcholinesterase (BChE) can cleave Cbl-G/CB[7] complex into two parts, i.e. the anti-cancer drug chlorambucil (Cbl) and a complex of NIR and CB[7]. Importantly, the fluorescence of NIR enhanced about 4.3 times in the presence of CB[7]. Cell assay experiments demonstrated that this supramolecular prodrug system exhibited excellent targeting ability to preferentially enter CD44 and RHAMM over-expressing A549 and HeLa cells and thus led to significant drug accumulation in cancer cells via receptor-mediated endocytosis. After incubating with butyrylcholinesterase, it could effectively kill tumor cells (A549 and HeLa), accompanied by the negligible side effects to normal cells. After

the ester bond of supramolecular prodrug was cleaved by butyrylcholinesterase, the emitted near-infrared light could realize the NIR cell imaging and thus monitor the drug release. Consequently, the obtained supramolecular prodrug system provides a novel strategy for simultaneous targeted cellular imaging and controlled drug release at specific sites that may have great potential applications in cancer therapy.



Scheme 1. Illustration of the construction of supramolecular prodrug and their enzyme-responsive

Cbl-G were prepared by the esterification reaction of the G and Cbl. G were synthesized according to the reported methods¹². The structures of G and Cbl-G were characterized by NMR and mass spectroscopy (Fig. S1-S10). First, the stoichiometry of Cbl-G/CB[7] complex was investigated by Job's plot and mass spectrum analysis, and the result showed a 1 : 1 binding stoichiometry (Fig. S11 and S12). Accordingly, the binding constant was determined to be $1.3 \times 10^5 \text{ M}^{-1}$ (Fig. S13). Similar 1 : 1 binding stoichiometry was also observed for the complexation of CB[7] with G (Fig. S14 and S15), and the association constant of G/CB[7] was determined to be $6.4 \times 10^5 \text{ M}^{-1}$ by using fluorescence titration (Fig. S16). These results suggested that G can be efficiently included in the hydrophobic cavity of CB[7] to form a stable host-guest complexes. Moreover, 2D ROESY experiment also provided the evidence for the inclusion complexation (Fig. S17), showing the clear NOE correlation between CB[7] and pyridinium group of G moiety. It has been well-established that CB[7] can complex with guests with positive charge. There are one positive charged pyridinium groups in G and Cbl-G molecule all. Due to the low solubility at high concentration of Cbl-G, we measured the NMR spectra of G, CB[7] and the host-guest complex to identify the host-guest property. As shown in (Fig. S18), peaks related to protons $H_{a,c,d,e,f,g,h,j}$ shifted upfield and broaden owing to inclusion into CB[7], which indicates that pyridinium groups in G complexing with CB[7].

Taking advantage of the strong host-guest interaction between pyridinium group and CB[7], the Cbl-G/CB[7] supramolecular complex can be easily constructed by simply mixing Cbl-G and CB[7] in aqueous solution. The high-resolution transmission electron microscopy (TEM) image gave the morphological information of Cbl-G/CB[7] as disordered nanofibers (Fig. 1a). However, when an equimolar amount of HA was added, the TEM image of Cbl-G/CB[7]/HA showed a number of homogeneous spherical nanoparticles with an average diameter of ca. 200 nm (Fig. 1b). Moreover, the hydrodynamic

diameter of Cbl-G/CB[7]/HA assembly obtained from the DLS experiment (Fig. 1f) was ca. 250 nm with a narrow distribution, which was basically consistent with the results of TEM. In addition, the zeta potential (Fig. 1e) of Cbl-G/CB[7]/HA assembly was measured to be ca. -3.23 mV. The negatively charged surface of assembly would facilitate its stability and biocompatibility in biological environments and thus extend its circulation time in vivo.¹³ The loading efficiency of Cbl-G in assembly was calculated to be as high as 98.2% from the UV/vis standard curve of Cbl-G (Fig. S26). In addition, the Cbl-G/CB[7]/HA assembly kept well dispersed in aqueous solution for one month, which demonstrated a good stability (Fig. S25).

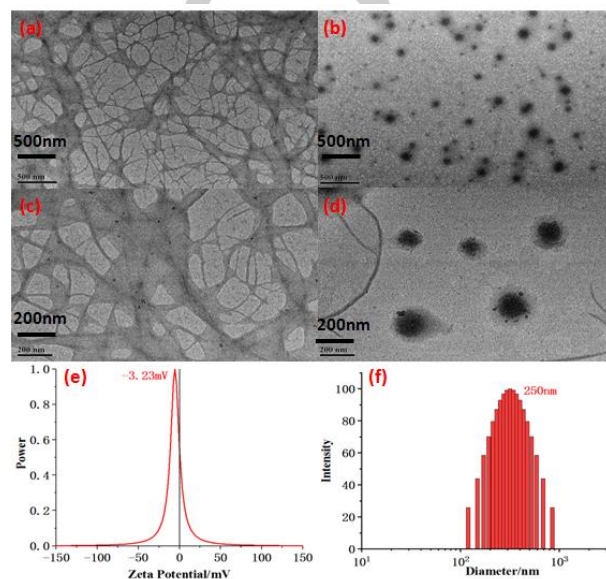


Figure 1. (a) TEM image of Cbl-G/CB[7], (b) TEM image of Cbl-G/CB[7]/HA, (c) enlarged image of (a), (d) enlarged image of (b), (e) zeta potential and (f) DLS of Cbl-G/CB[7]/HA. [Cbl-G] = CB[7] = 0.05 mM, [HA] = 15 mg/ml.

In order to confirm the presumed concomitant release of fluorophore and Cbl, we monitored the responsive spectroscopic change of assembly in the presence of BChE. As shown in Fig. 2, the time-dependent fluorescence emission changes of Cbl-G, Cbl-G/CB[7] and Cbl-G/CB[7]/HA were recorded after the addition of BChE at 37 °C. Without BChE, Cbl-G, Cbl-G/CB[7] or Cbl-G/CB[7]/HA barely fluoresced. After the addition of BChE, the fluorescence of Cbl-G at 652 nm showed a smooth enhancement, but the fluorescence of Cbl-G/CB[7] or Cbl-G/CB[7]/HA rapidly increased with time. After 7 h, the fluorescence emission intensity of Cbl-G/CB[7] or Cbl-G/CB[7]/HA was 4.3 times higher than that of Cbl-G. The increased fluorescence of Cbl-G was owing to the cleavage of ester bond in Cbl-G and the subsequent release of G, which was accompanied by the simultaneous release of a Cbl drug molecule. Therefore, we can calculate the drug release rate as 96.15% according to the increase of fluorescence intensity. Furthermore, no spherical aggregates can be observed in TEM images after treating the Cbl-G/CB[7]/HA assembly with BChE (Fig. S18). This obvious NIR fluorescence endowed the assembly with the ability of real-time tracking of drug delivery and intracellular imaging, suggesting that the assembly might be of potential application value in cancer diagnosis. It is worth noting that the main role of hyaluronic acid here is to act

as a targeting agent for targeted cell imaging, and thus hyaluronic acid does not cause significant changes in fluorescence.

Moreover, mass-spectrometric detection is also carried out to validate the enzymatic cleavage of the ester bonds of Cbl-G in the supramolecular nanoparticles. In the mass spectra of supramolecular nanoparticles at different time intervals (Fig. S19), the m/z peak of [Cbl-G/CB[7]-I] at 1807.6 gradually decreased while the peak of [G/CB[7]-I] at 1522.6 gradually increased after 6h (Fig. S21) after the addition of BChE, indicating the cleavage of ester bond. These results jointly indicated that the anti-cancer drug Cbl was indeed released from the designed drug delivery system through BChE-responsive breaking of the ester bond. However, there are still some Cbl-G molecules that are not enzymatically hydrolyzed. A possible reason may be that the Cbl-G molecules are stacked closely in the assembly, and some of them are being enveloped in the cavity of CB[7], which hinders the attack of BChE to some extent. Subsequently, the specificity of BChE-responsive disassembly was also investigated. The Cbl-G/CB[7]/HA solution showed no significant changes of fluorescence intensity at 652 nm when using other enzymes, such as trypsin (Fig. S23) and glucose oxide (Fig. S24) instead of BChE, demonstrating that the Cbl-G/CB[7]/HA system exhibited a high specificity towards BChE.

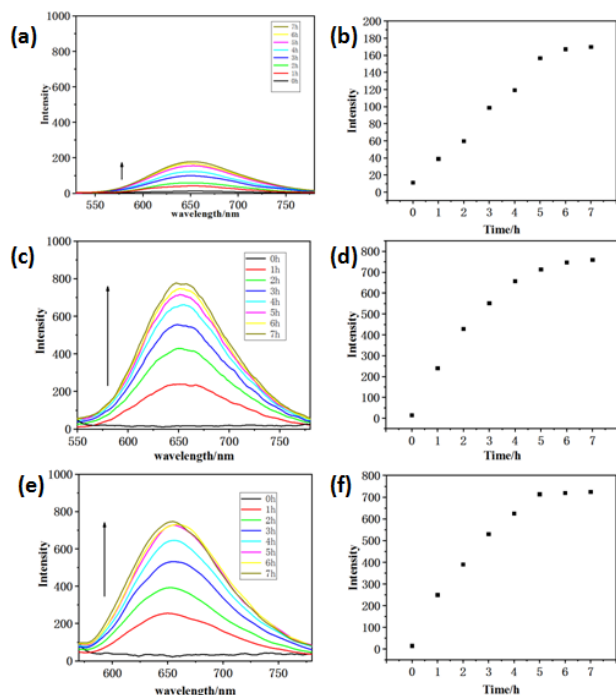


Figure 2. Fluorescence emission spectra of Cbl-G (a), Cbl-G/CB[7] (c), Cbl-G/CB[7]/HA (e) at different time within 7h in the presence of 1U/mL BChE. (b) Time-dependent changes of fluorescence intensity at 652 nm for Cbl-G (b), Cbl-G/CB[7] (d), Cbl-G/CB[7]/HA (f) in the presence of 1U/mL BChE. [Cbl-G] = CB[7] = 0.05 mM, λ_{exc} = 400 nm, [BChE] = 0.5mg/ml

The cytotoxicity experiments were also performed to evaluate the anticancer activities of Cbl-G/CB[7]/HA assembly by using A549 and HeLa cells as models. As shown in Fig. 3a, negligible influence on the relative cell viability was observed in the presence of free HA or CB[7] at the tested concentrations. With respect to the prodrug assembly, the relative cell viability of the group with BChE (1U/ml) was twice lower than that of the group without BChE (1U/ml), indicating that the assembly had significant enzyme responsiveness and excellent anti-cancer activity. However, when the

receptors on the A549 and HeLa cell surface were blocked by an excess amount of HA, the cancer cell inhibition of assembly decreased distinctly, and the relative cellular viability was measured as 62.1%. This phenomenon indicated that the interaction of HA with the HA receptor played an important role in the internalization of assembly into cancer cells.¹⁴ Moreover, the side effect of assembly was also evaluated by using HA receptor negative 293T normal cells. As shown in Fig. 3b, due to the lack of HA receptor on the surface of normal cells, the assembly could be hardly internalized into cytoplasm of 293T cells and showed the high cellular viability as 90%. Furthermore, HA and CB[7] showed no cytotoxicity to normal cells. Therefore, we can deduce that the assembly could enter the cancer cells via the HA receptor mediated endocytosis effect and showed a good malignant cell inhibition effect but much lower side effects in normal cells.

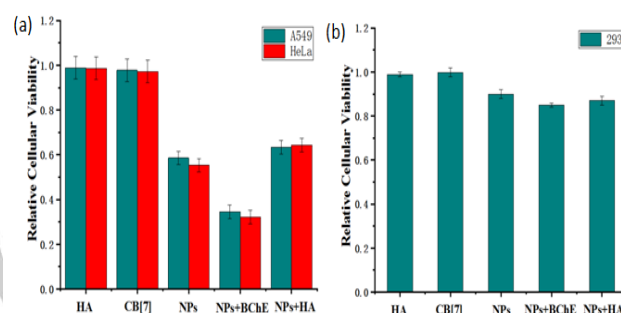


Figure 3. Relative cellular viability of A549 tumor cells, HeLa cells (a) and 293T cells (b) (CB[7] = [Cbl-G] = 100 μ M)

After verifying the anti-cancer effect of assembly, we also investigated its imaging capability before and after enzyme response. As shown in Figure 4, after incubated with Cbl-G/CB[7]/HA assembly for 12 h, A549 cells (human lung adenocarcinoma cells) exhibited bright red fluorescence in the presence of BChE. In contrast, no fluorescence was observed in the case without BChE.

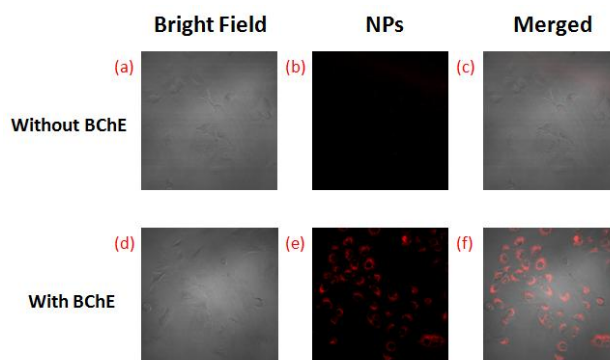


Figure 4. Confocal laser scanning microscopy images of enzyme-responsive cellular imaging of A549 cells when incubated without and with BChE after 12 hours.

In conclusion, an enzyme-responsive supramolecular prodrug for targeted cellular imaging and controlled drug release was constructed. The obtained supramolecular prodrug had a hydrophilic and biocompatible HA shell, which could recognize and target HA receptor

overexpressed cancer cells, and exhibiting satisfactory stimulus-responsive drug release and fluorescence changes for real-time tracking of drug delivery and cellular imaging under BChE. Moreover, the results of cytotoxicity experiments proved that supramolecular prodrug could be internalized into cancer cells by HA receptor mediated endocytosis. The advantages of is strategy include (1) it can improve the water solubility of anti-cancer drugs and realize targeting ability, (2) drug release can be controlled by enzyme response, (3) NIR fluorophore could allow us to visualizing cancer cell and real-time tracking drug release. We believe that this butyrylcholinesterase-responsive supramolecular prodrug may provide new therapeutic options to enhance the basic chemotherapeutic approach.

Acknowledgements

This work was supported by the National Natural Science Foundation of China (Grants 21971127, 21772099, and 21861132001).

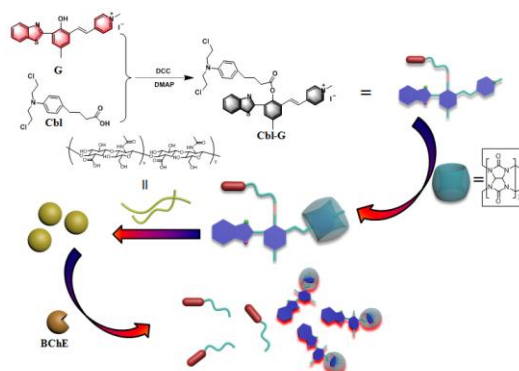
Keywords: cellular imaging • cucurbit[n]urils • enzyme responsive • hyaluronic acid • supramolecular prodrug

- [1] a) X. Guan, Y. Chen, X. Wu, P. Li and Y. Liu, *Chem. Commun.* **2019**, 55, 953-956; b) D.-S. Guo, K. Wang, Y.-X. Wang and Y. Liu, *J. Am. Chem. Soc.* **2012**, *134*, 10244-10250; c) G. K. Such, Y. Yan, A. P. R. Johnston, S. T. Gunawan and F. Caruso, *Adv. Mater.* **2015**, *27*, 2278-2297; d) A. Tanaka, Y. Fukuoka, Y. Morimoto, T. Honjo, D. Koda, M. Goto and T. Maruyama, *J. Am. Chem. Soc.* **2015**, *137*, 770-775; e) J.-H. Liu, X. Wu, Y.-M. Zhang, and Y. Liu, *Asian J. Org. Chem.* **2018**, *7*, 2444-2447; f) X. Han, Y. Chen, H.-L. Sun, Y. Liu, *Asian J. Org. Chem.* **2018**, *7*, 870-874.
- [2] a) W.-C. Geng, J. L. Sessler and D.-S. Guo, *Chem. Soc. Rev.* **2020**, *49*, 2303-2315; b) M. J. Webber and R. Langer, *Chem. Soc. Rev.* **2017**, *46*, 6600-6620; c) J. Zhou, G. Yu and F. Huang, *Chem. Soc. Rev.* **2017**, *46*, 7021-7053.
- [3] a) M. H. Lee, J. L. Sessler and J. S. Kim, *Acc. Chem. Res.* **2015**, *48*, 2935-2946; b) Yu, Wei Yu, Z. Mao, C. Gao and F. Huang, *small.* **2015**, *11*, 919-925; c) Q. Yu, Y.-M. Zhang, Y.-H. Liu, X. Xu and Y. Liu, *Sci. Adv.* **2018**, *4*, 2297; d) J. H. Lee, K. J. Chen, S. H. Noh, M. A. Garcia, H. Wang, W. Y. Lin and H. R. Tseng, *Angew. Chem. Int. Ed.* **2013**, *52*, 4384-4388; e) Q. Duan, Y. Cao, Y. Li, X. Hu, T. Xiao, C. Lin, Y. Pan and L. Wang, *J. Am. Chem. Soc.* **2013**, *135*, 10542-10549.
- [4] a) S. J. Barrow, S. Kasera, M. J. Rowland, J. Barrio and O. A. Scherman, *Chem. Rev.* **2015**, *115*, 12320-12406; b) Y.-H. Liu, Y.-M. Zhang, H.-J. Yu and Y. Liu, *Angew. Chem. Int. Ed.* **2020**, *59*, 2-13.
- [5] a) R. Dhiman, S. Pen, P. K. Chandrakumar, T. J. Frankcombe and A. I. Day, *Chem. Commun.* **2020**, 56, 2529-2537; b) H. Zou, J. Liu, Y. Li, X. Li and X. Wang, *small.* **2018**, *14*, 1802234.
- [6] a) D. Shetty, J. K. Khedkar, K. M. Park and K. Kim, *Chem. Soc. Rev.* **2015**, *44*, 8747-8761; b) W. Liu, S. K. Samanta, B. D. Smith and L. Isaacs, *Chem. Soc. Rev.* **2017**, *46*, 2391-2403.
- [7] X.-M. Chen, Y. Chen, Q. Yu, B.-H. Gu and Y. Liu, *Angew. Chem. Int. Ed.* **2018**, *57*, 12519-12523.
- [8] a) D. Mao, Y. Liang, Y. Liu, X. Zhou, J. Ma, B. Jiang, J. Liu and D. Ma, *Angew. Chem. Int. Ed.* **2017**, *56*, 12614-12618; b) S. K. Samanta, J. Quigley, B. Vinciguerra, V. Briken and L. Isaacs, *J. Am. Chem. Soc.* **2017**, *139*, 9066-9074.
- [9] a) Y. Yang, Y.-J. Jin, X. Jia, S.-K. Lu, Z.-R. Fu, Y.-X. Liu and Y. Liu, *ACS Med. Chem. Lett.* **2020**, *11*, 451-456; b) H. Kim, M. Shin, S. Han, W. Kwon and S. K. Hahn, *Biomacromolecules.* **2019**, *20*, 2889-2903; c) Q. Yu, B. Zhang, Y.-M. Zhang, Y.-H. Liu and Y. Liu, *ACS Appl. Mater. Interfaces.* **2020**, *12*, 13709-13717.
- [10] X.-Y. He, X.-H. Ren, Y. Peng, J.-P. Zhang, S.-L. Ai, B.-Y. Liu, C. Xu and S. X. Cheng, *Adv. Mater.* **2020**, *32*, 2000208.
- [11] a) A. C. Sedgwick, L. Wu, H.-H. Han, S. D. Bull, X.-P. He, T. D. James, J. L. Sessler, B. Tang, H. Tian and J. Yoon, *Chem. Soc. Rev.* **2018**, *47*, 8842-8880; b) K. Wu, T. Zhang, Z. Wang, L. Wang, L. Zhan, S. Gong, C. Zhong, Z.-H. Lu, S. Zhang and C. Yang, *J. Am. Chem. Soc.* **2018**, *140*, 8877-8886; c) P. Zhou and K. Han, *Acc. Chem. Res.* **2018**, *51*, 1681-1690.
- [12] a) C. Chang, F. Wang, J. Qiang, Z. Zhang, Y. Chen, W. Zhang, Y. Wang, X. Chen, *Sens. Actuators B: Chem.* **2017**, *243*, 22-28; b) T. Chen, T. Wei, Z. Zhang, Y. Chen, J. Qiang, F. Wang, X. Chen, *Dyes Pigments.* **2017**, *140*, 392-398; c) Y. Chen, T. Wei, Z. Zhang, W. Zhang, J. LV, T. Chen, B. Chi, F. Wang, X. Chen, *Chinese. Chem. Lett.* **2017**, *28*, 1957-1960.
- [13] a) X. Sun, Gui. He, Chu. Xiong, Chen. Wang, X. Lian, L. Hu, Z. Li, S. Dalgarno, Y.-W. Yang and J. Tian, *ACS Appl. Mater. Interfaces.* **2021**, *13*, 3679-3693; b) Y. Liu, Y. Liao, P. Li, Z.-T. Li and D. Ma, *ACS Appl. Mater. Interfaces.* **2020**, *12*, 7974-7983; c) B. Shi, N. Ren, L. Gu, G. Xu, R. Wang, T. Zhu, Y. Zhu, C. Fan, C. Zhao and H. Tian, *Angew. Chem. Int. Ed.* **2018**, *58*, 16826-16830; d) Q. Guo, G. Li, M. Rao, L. Wei, F. Gao, W. Wu, Q. Yang, G. Cheng and C. Yang, *Dyes and Pigments.* **2020**, *182*, 10864.
- [14] a) Luo, Y and Prestwich, G. D, *Bioconjugate Chem.* **1999**, *10*, 755-763; b) Luo, Y, Ziebell, M. R and Prestwich, G. D, *Biomacromolecules.* **2000**, *1*, 208-218; c) Lee, H, Lee, K and Park, T. G. *Bioconjugate Chem.* **2008**, *19*, 1319-1325.

Table of Contents

Butyrylcholinesterase responsive supramolecular prodrug with targeted near-infrared cellular imaging property

Yonghui Sun, Yong Chen, Xianyin Dai and Yu Liu*



An enzyme responsive supramolecular prodrug with near-infrared targeted cell imaging property was successfully constructed. Cell experiments indicated that the prodrug nanoparticles are easily internalized into cancer cells via receptor-mediated endocytosis, and disassembled under the action of butyrylcholinesterase by cutting the ester bond of prodrug, exhibiting a controlled drug release behavior as well as a simultaneous near-infrared (NIR) fluorescence imaging in cancer cells.